

# Catalysis Science & Technology

Accepted Manuscript



This is an *Accepted Manuscript*, which has been through the Royal Society of Chemistry peer review process and has been accepted for publication.

*Accepted Manuscripts* are published online shortly after acceptance, before technical editing, formatting and proof reading. Using this free service, authors can make their results available to the community, in citable form, before we publish the edited article. We will replace this *Accepted Manuscript* with the edited and formatted *Advance Article* as soon as it is available.

You can find more information about *Accepted Manuscripts* in the [Information for Authors](#).

Please note that technical editing may introduce minor changes to the text and/or graphics, which may alter content. The journal's standard [Terms & Conditions](#) and the [Ethical guidelines](#) still apply. In no event shall the Royal Society of Chemistry be held responsible for any errors or omissions in this *Accepted Manuscript* or any consequences arising from the use of any information it contains.



## Towards understanding the hydrodeoxygenation pathways of furfural-acetone aldol condensation products over supported Pt catalysts

R. Ramos, Z. Tišler, O. Kikhtyanin and D. Kubička\*

Received 00th January 20xx,  
Accepted 00th January 20xx

DOI: 10.1039/x0xx00000x

[www.rsc.org/](http://www.rsc.org/)

Aiming at the valorisation of furfural-derived compounds, the hydrodeoxygenation of furfural acetone condensation products has been studied using platinum supported catalysts. The influence of the catalytic properties of different supports, such as; SiO<sub>2</sub>, Al<sub>2</sub>O<sub>3</sub>, TiO<sub>2</sub>, hydrotalcite (HTC), Beta zeolite, Al-SBA-15 and WO<sub>3</sub>-ZrO<sub>2</sub>, was evaluated in a batch reactor for 480 min at 200 °C and 50 bar of H<sub>2</sub>. The used feed consisted of a mixture of furfural-acetone adducts (C<sub>8</sub>-C<sub>19</sub>), obtained in previous experiments using a continuous flow reactor and hydrotalcite as a catalyst. Except the Pt/SiO<sub>2</sub>, all catalysts showed a high conversion of the reactants, especially due to the hydrogenation of all the aliphatic C=C bonds. However, the extent of further hydrogenation (furan C=C and ketone C=O bonds) was limited, particularly when using HTC and Al<sub>2</sub>O<sub>3</sub> as a support. The higher accessibility of Pt/TiO<sub>2</sub> and the smaller Pt particle size showed by Pt/Al-SBA-15, Pt/WO<sub>3</sub>-ZrO<sub>2</sub> and Pt/Beta in comparison with the other catalysts, led to an improvement in the hydrogenation of furanic and ketonic groups, likely due to lower adsorption constraints. The higher acid character of the latter group of catalysts promotes dehydration and ring opening steps, enhancing thus the selectivity towards linear alcohols. Likewise, a significant increase in the extent of aldol condensation reactions was also observed with these catalysts, yielding longer carbon chains compounds. Based on this study, a reaction scheme for the transformation of 4-(2-furyl)-3-buten-2-one (C<sub>8</sub>) into octane has been proposed in order to establish a valuable correlation between the main conversion pathways and the catalytic properties of the employed heterogeneous catalyst contributing thus to further development of efficient deoxygenation catalysts.

### Introduction

An efficient conversion of lignocellulose-derived platform compounds, such as furfural or hydroxymethylfurfural, into liquid fuels and value-added chemicals could contribute to the development of more sustainable and environmentally-friendly alternative renewable sources and energy technologies.<sup>1,2</sup> Furfural (C<sub>5</sub>H<sub>4</sub>O<sub>2</sub>) is an oxygenated compound obtained through dehydration of the hemicellulose building blocks (e.g., xylose and arabinose), that are derived from lignocellulosic biomass by acid-catalyzed treatments.<sup>3</sup> Since lignocellulose is the main component of agricultural wastes and forest residues, the synthesis and the subsequent transformation of furfural (and its derivatives) has become an active research area in recent years.<sup>3-5</sup> However, the carbon chain length of furfural, once hydrodeoxygenated, is in general too short for fuel applications. In this respect, aldol condensation of furfural with small ketones affords larger organic molecules (≥C<sub>8</sub>) by forming C–C bonds between carbonyl-containing compounds. Recently, this strategy has been proposed for the direct condensation of furfural (F) with acetone (Ac) as a promising approach to yield alkanes precursors.<sup>6-10</sup> Accordingly, the formation of F-Ac monomer (C<sub>8</sub>) and F<sub>2</sub>-Ac dimer (C<sub>13</sub>) mostly takes place in

presence of base or acid catalyst at low temperatures (25–70 °C). It should be noted that acetone itself is also available from renewable biomass through fermentation<sup>11</sup> or ketonization strategies.<sup>12,13</sup>

In order to yield valuable liquid hydrocarbons, furfural-acetone condensate products have to be deoxygenated, typically at high hydrogen pressures (20–80 bar) and mild temperatures (170–300 °C). During deoxygenation, the furfural-acetone adducts are subjected to hydrogenation, ring opening and dehydration reactions, yielding numerous intermediate products according to diverse reaction pathways.<sup>10,14-16</sup> Some authors have studied deoxygenation of furfural-acetone condensation adducts into alkanes as one step process using bifunctional catalysts.<sup>15-17</sup> However, due to the complexity of this process, the majority of authors suggest carrying out the hydrogenation step individually, i.e. as an intermediary transformation step between the aldol condensation reaction and the final deoxygenation stage.<sup>10,14,18-20</sup>

The hydrogenation of furfural-acetone aldol condensation products plays an important role in the multi-step catalytic transformation into liquid alkanes as it increases the feedstock stability as a result of the elimination of the unsaturated monomer and dimer (F-Ac and F<sub>2</sub>-Ac, respectively). Consequently, the stabilization allows more severe deoxygenation reaction conditions and thus better yields of alkanes, i.e. fully deoxygenated products. In this sense, there are three different kinds of double bonds to be hydrogenated: aliphatic C=C, furanic C=C and ketonic C=O bonds. Thermodynamic and kinetic considerations favour hydrogenation of the C=C bond over C=O,<sup>21,22</sup> whereas steric constraints usually limit

Research Institute of Inorganic Chemistry, RENTECH-UniCRE, Chempark Litvínov, Záluží-Litvínov, 436 70, Czech Republic  
E-mail: David.Kubicka@vuanch.cz;

the hydrogenation rates of C=C in comparison with C=O hydrogenation.<sup>23</sup> Moreover, the furanic ring of furfural may also cause steric hindrance, reducing the hydrogenation of the C=C furanic ring compared to the aliphatic C=C bonds.<sup>24</sup> Similarly, the hydrogenation of the furanic C=O bond is generally more restricted, inhibiting ring opening reactions which are a fundamental step towards the formation of linear alcohols.<sup>25</sup>

The selection of the catalyst plays a critical role in the conversion pathways. Among the different metal phases studied, platinum has been revealed as one of the most suitable metals for hydrogenating both double bonds and ketone bonds, at moderate temperatures and pressures.<sup>17,26</sup> Concerning the support, its main function is to achieve the optimum dispersion, to stabilize suitably the metal species and to provide sufficient mass transfer rates, i.e. the consideration of the textural properties of the supports is crucial. Additionally, support materials can exhibit acidic or basic properties, which promote different reactions and intermediates formation, altering efficiency, and therefore, changing the overall activity and selectivity of the transformation.<sup>26</sup>

Within this context, the main scope of this contribution is to investigate the influence of different supported platinum catalysts on the deoxygenation of furfural-acetone condensation products. The research is focused on the use of real furfural-acetone aldol condensation products obtained in large scale using a flow reactor and basic hydrotalcite as a catalyst.<sup>27</sup> The activity of seven different supports (SiO<sub>2</sub>, Al<sub>2</sub>O<sub>3</sub>, TiO<sub>2</sub>, hydrotalcite, Beta zeolite, Al-SBA-15 and WO<sub>3</sub>-ZrO<sub>2</sub>) loaded with platinum was compared at 200 °C and 50 bar. The support selection covers a wide range of acidity and textural properties, allowing to evaluate the effect of active sites nature and pore morphology on the reaction mechanism. The understanding of this conversion is particularly useful for the design of novel catalysts that will allow developing a competitive technology for the production of valuable alkanes from furfural condensation adducts.

## Experimental

### Feedstock.

The used feed consisted of a mixture of furfural-acetone aldol condensation products obtained from the experiments described elsewhere,<sup>27</sup> using a continuous flow fixed bed reactor at 50 °C and hydrotalcite (Mg/Al=3) as a catalyst. The aldol condensation reactions of furfural and acetone led to the formation of a heterogeneous mixture of compounds, resulting from the cross aldol condensation of the aldehyde and the ketone groups, but also from acetone self-condensation affording diacetone alcohol (DAA) and mesityl oxide (MSO). In order to achieve a more appropriate ratio between the reactant molecules (F-Ac and derivatives, i.e. various aldol condensation products) and the amount of catalyst, the initial feed was diluted by adding more acetone. Thus, the final feedstock loaded into the batch reactor consisted of 50 ml of aldol condensation products and 100 ml of acetone. The molar concentration of the main compounds present in the feedstock (X<sub>i</sub>), determined by GC and GC-MS analyses, is given in Table 1.

**Table 1** Composition of the used feedstock

Compound	Molecular mass (g/mol)	Molar fraction (X <sub>i</sub> )
Acetone	58	9.7·10 <sup>-1</sup>
DAA	116	3.86·10 <sup>-3</sup>
MSO	98	2.48·10 <sup>-4</sup>
F-Ac	136	1.95·10 <sup>-2</sup>
F-Ac <sub>2</sub>	176	2.06·10 <sup>-3</sup>
F <sub>2</sub> -Ac	214	2.71·10 <sup>-3</sup>
(F-Ac) <sub>2</sub>	272	5.79·10 <sup>-4</sup>
F <sub>2</sub> -Ac <sub>2</sub>	254	1.35·10 <sup>-3</sup>
F <sub>2</sub> -Ac <sub>3</sub>	294	7.34·10 <sup>-4</sup>

### Catalysts preparation.

Different supports were used for studying the effect of their catalytic properties on the deoxygenation of furfural-acetone adducts. The influence of their textural and acido-basic properties was evaluated by investigating a wide range of materials including commercial supports SiO<sub>2</sub> (Astin Catalysts and Chemicals), Al<sub>2</sub>O<sub>3</sub> (Astin Catalysts and Chemicals), TiO<sub>2</sub> (Euro Support), Beta zeolite (Zeolyst Int., Si/Al=12.5), WO<sub>3</sub>-ZrO<sub>2</sub> (Euro Support), and in-house synthesized hydrotalcite<sup>27</sup> and Al-SBA-15 (Si/Al=50).

The incorporation of platinum to the supports was carried out by wetness-impregnation of tetraammine-platinum(II) nitrate (Pt(NH<sub>3</sub>)<sub>4</sub>(NO<sub>3</sub>)<sub>2</sub>) to prepare catalysts with a nominal metal loading in the range 0.2-0.8 wt.%. The deposition of the Pt was carried out by adding an aqueous solution of the precursor to the supports. After impregnation, the catalysts were dried at 120 °C overnight and then calcined at 500 °C in air for 6 h (heating rate 1 °C·min<sup>-1</sup>).

### Catalysts characterization.

The catalysts were characterized by different physico-chemical characterization methods in order to determine their main textural and acido-basic properties.

Textural properties were measured using nitrogen adsorption-desorption isotherms at 77 K with a Quantachrome AUTOSORB instrument. Prior to the analyses, the samples were treated at 250 °C for 3 h under nitrogen flow in order to remove adsorbed compounds. The BET equation was used for the specific surface area calculation, whereas the pore volume and pore size were determined by the BJH method.

The acidic and basic properties of the catalysts were evaluated by temperature programmed desorption (TPD) of ammonia and carbon dioxide, respectively, in a Micromeritics Autochem 2950 apparatus. Prior to the TPD analyses, catalyst samples were reduced in situ under 10 vol.% H<sub>2</sub>/Ar (25 cm<sup>3</sup>·min<sup>-1</sup>) at 350 °C (10 °C·min<sup>-1</sup>) for 60 min to reproduce the condition of the catalyst at the beginning of the catalytic experiments. Before reduction, the sample is outgassed under a He flow of 25 cm<sup>3</sup>·min<sup>-1</sup> with a heating ramp of 10 °C·min<sup>-1</sup> up to 500 °C.

The NH<sub>3</sub> TPD experiments were started by cooling the sample after reduction down to 180 °C followed by treating it with an ammonia stream (10 vol.% in He) of 25 cm<sup>3</sup>·min<sup>-1</sup> for 30 min. Once the sample was saturated, the physically adsorbed NH<sub>3</sub> was removed

by flowing He ( $25 \text{ cm}^3\cdot\text{min}^{-1}$ ) for 60 min. Finally, temperature programmed desorption was performed subjecting the sample to a heating rate of  $15 \text{ }^\circ\text{C}\cdot\text{min}^{-1}$  in flowing He ( $25 \text{ cm}^3\cdot\text{min}^{-1}$ ) up to  $500 \text{ }^\circ\text{C}$ , maintaining this temperature for 30 min.

In case of the  $\text{CO}_2$  TPD analyses, the sample was cooled after reduction down to  $50 \text{ }^\circ\text{C}$  and saturated under a  $\text{CO}_2$  flow (10 vol.% in He) of  $50 \text{ cm}^3\cdot\text{min}^{-1}$  for 30 min. Subsequently, the physically adsorbed carbon dioxide was removed by flowing He ( $25 \text{ cm}^3\cdot\text{min}^{-1}$ ) at  $50 \text{ }^\circ\text{C}$  for 60 min. Finally, the chemically absorbed  $\text{CO}_2$  was desorbed by heating up the sample to  $850 \text{ }^\circ\text{C}$  (heating rate of  $15 \text{ }^\circ\text{C}\cdot\text{min}^{-1}$ ) in flowing He ( $25 \text{ cm}^3\cdot\text{min}^{-1}$ ) and maintaining this temperature for 30 min. The amounts of desorbed species were quantified using calibration standards.

The platinum content of the catalysts was determined by X-ray Fluorescence Spectroscopy (XRF) using a Philips PW 1404 UniQuant apparatus. The reducibility of the Pt phase was examined by temperature-programmed reduction (TPR) using a Micromeritics Autochem 2950 unit. Catalyst samples of 0.1 g were pretreated at  $500 \text{ }^\circ\text{C}$  in flowing Ar ( $25 \text{ cm}^3\cdot\text{min}^{-1}$ ) for 60 min, then cooled down to  $40 \text{ }^\circ\text{C}$ , and finally reduced under a stream of 10 vol.%  $\text{H}_2/\text{Ar}$  ( $25 \text{ cm}^3\cdot\text{min}^{-1}$ ) while increasing the temperature by  $10 \text{ }^\circ\text{C}\cdot\text{min}^{-1}$  up to  $500 \text{ }^\circ\text{C}$ .  $\text{H}_2$  uptake as a function of temperature was measured on-line using a TCD detector.

The metal dispersion and particle size were determined by CO pulse chemisorption at  $50 \text{ }^\circ\text{C}$ . Prior to the chemisorption, the samples were reduced in situ under 10 vol.%  $\text{H}_2/\text{Ar}$  ( $20 \text{ cm}^3\cdot\text{min}^{-1}$ ) at  $350 \text{ }^\circ\text{C}$ . After reduction, the sample was cooled down to  $50 \text{ }^\circ\text{C}$  and then 5 vol.%  $\text{CO}/\text{He}$  gas was introduced by pulse dosing in a He flow ( $50 \text{ cm}^3\cdot\text{min}^{-1}$ ). Metal dispersion was determined by measuring the amount of adsorbed CO, sample metal loading and using the adsorption stoichiometry factor 1 ( $\text{M} + \text{CO} \rightarrow \text{M-CO}$ ).

### Catalytic experiments.

The performance of the catalysts was studied in a high-pressure 300 ml batch reactor (Parr Instrument Co.) equipped with digital controllers of stirring speed, temperature and pressure and gas flowmeters. All data were collected and monitored continuously during the reaction by a Parr 4848B acquisition interface.

Prior to the reaction, the catalyst (1 g) was reduced in situ by  $\text{H}_2$  flow ( $80 \text{ cm}^3\cdot\text{min}^{-1}$ ) at  $350 \text{ }^\circ\text{C}$  for 90 min. After cooling down, the reactor was loaded with 150 ml of the feedstock mixture described above (Table 1) and purged thoroughly with hydrogen. Subsequently, heating of the reactor was performed under moderate conditions - pressure (15 bar) and stirring (100 rpm). Once the desired temperature ( $200 \text{ }^\circ\text{C}$ ) was reached, the vessel was pressurized to 50 bar of  $\text{H}_2$  and the stirring speed was increased to 1000 rpm to prevent external mass transfer limitations. The samples of products were collected at different intervals during the course of the reaction (480 min) in order to evaluate the kinetic behaviour. The product mixtures were analyzed by an Agilent 7890A GC unit equipped with a flame ionization detector (FID) using a HP-5 capillary column (30 m, 0.32 ID,  $0.25 \mu\text{m}$ ). The hydrogenated products were identified by using standard reference compounds along with GC-MS analyses using Thermo Scientific ITQ 1100 unit.

The evolution of the concentrations of the reactants and products, and the yields of the products were calculated using GC analysis of the feedstock and the liquid product samples as follows:

$$[X_i]_t\% = \frac{[X_i]_t}{[X_i]_{t=0}} \cdot 100$$

$$[Y_i]_t\% = \frac{[X_i]_t - [X_i]_{t=0}}{[X_{F-Ac}]_{t=0}} \cdot 100$$

Where  $[X_i]_t\%$  represents the relative molar concentration of the specie  $i$  at time  $t$ ,  $[X_i]_t$  is the molar concentration of  $i$ ,  $[Y_i]_t\%$  is the yield of the specie  $i$  (derived from F-Ac) at time  $t$  and  $[X_{F-Ac}]_{t=0}$  is the molar concentration of the compound F-Ac ( $\text{C}_8$ ) at the beginning of the reaction.

## Results and discussion

### Catalysts properties.

The catalysts prepared by impregnation of platinum on different supports were characterized by a number of techniques in order to determine their main physico-chemical properties. The characterization results are summarized in Table 2.

The results of XRF analysis show a Pt content similar to the theoretical value from the starting solution, indicating that a complete incorporation of metal species has been achieved by the wetness-impregnation process. The textural properties of the samples present a wide variety of values, ranging from the low porosity shown by Pt/ $\text{SiO}_2$  ( $56 \text{ m}^2\cdot\text{g}^{-1}$ ) up to high specific surface area materials, such as Pt/Beta and Pt/Al-SBA-15 (529 and  $672 \text{ m}^2\cdot\text{g}^{-1}$ , respectively). The higher values of the BET surface area play an important role since they help to achieve a better platinum dispersion and metal interaction with the support, improving the metal sites activity. Similarly, the pore size values vary within a broad interval from microporous ( $6\text{-}7 \text{ \AA}$  in case of Pt/Beta) to mesoporous materials ( $30\text{-}300 \text{ \AA}$ ), which may affect considerably the accessibility of the reactant molecules to the active sites due to steric limitations. Thus, according to the data given in Table 2, Pt/ $\text{TiO}_2$  ( $302 \text{ \AA}$ ) should provide a good access to its active sites, whereas Pt/Beta zeolite, despite its remarkable specific surface, may suffer from major diffusional problems. Regarding pore volume, Pt/Al-SBA-15 shows the highest value ( $1.28 \text{ cm}^3\cdot\text{g}^{-1}$ ) due to the combination of high specific surface and pore size.

The acidity/basicity of the catalysts, as determined by  $\text{NH}_3/\text{CO}_2$  desorption, is included in Table 2. The total amount of acid/basic sites ( $\text{meq NH}_3/\text{CO}_2\cdot\text{g}^{-1}$ ) is related to the ammonia/carbon dioxide desorbed, whereas the maximum desorption temperature ( $T_{\text{max}}$ ) is an indication of the acid/basic sites strength. Pt/Al-SBA-15, Pt/ $\text{WO}_3\text{-ZrO}_2$  and Pt/Beta show the highest acidity; the remarkable acid character ( $0.648 \text{ meq NH}_3\cdot\text{g}^{-1}$ ) of the latter material is related to the low Si/Al ratio (12.5) of the BEA zeolite framework. Regarding the acid strength, these materials show a similar maxima value for the desorption temperature ( $268\text{-}271 \text{ }^\circ\text{C}$ ). Pt/ $\text{Al}_2\text{O}_3$  and Pt/ $\text{TiO}_2$  catalysts also exhibit acid character although in a lower range both in the amount ( $0.110\text{-}0.138 \text{ meq NH}_3\cdot\text{g}^{-1}$ ) and in the strength ( $238\text{-}240 \text{ }^\circ\text{C}$ )

**Table 2** Physicochemical properties of the studied catalysts

Catalyst	Pt content <sup>(a)</sup> (wt.%)	Pt dispersion <sup>(b)</sup> (%)	Pt particle size <sup>(b)</sup> (nm)	Active metal surface area <sup>(b)</sup> (m <sup>2</sup> /g)	S <sub>BET</sub> <sup>(c)</sup> (m <sup>2</sup> /g)	Pore volume <sup>(d)</sup> (cm <sup>3</sup> /g)	Pore size <sup>(d)</sup> (Å)	Acid/basic sites		
								(meq NH <sub>3</sub> /g) <sup>(e)</sup>	(meq CO <sub>2</sub> /g) <sup>(f)</sup>	T <sub>max</sub> (°C) <sup>(g)</sup>
Pt/SiO <sub>2</sub>	0.35	0.8	141.6	0.01	46	0.648	49	-	-	-
Pt/Al <sub>2</sub> O <sub>3</sub>	0.54	14.6	7.7	0.19	207	0.431	38	0.138	-	240
Pt/TiO <sub>2</sub>	0.48	7.9	14.3	0.09	77.6	0.403	302	0.110	0.160	238/110
Pt/HTC	0.73	3.8	29.4	0.07	179	0.730	31	-	0.796	110
Pt/Beta	0.48	34.6	3.2	0.42	529	0.116*	6-7*	0.648	-	271
Pt/Al-SBA-15	0.29	65.3	1.7	0.47	672	1.283	78	0.221	-	261
Pt/WO <sub>3</sub> -ZrO <sub>2</sub>	0.08	41.4	2.7	0.08	90.3	0.272	78	0.258	-	268

<sup>(a)</sup> XRF measurements.<sup>(b)</sup> CO pulse chemisorption at 50 °C of samples reduced at 350 °C.<sup>(c)</sup> Nitrogen adsorption at 77 K.<sup>(d)</sup> BJH method.<sup>(e)</sup> NH<sub>3</sub> TPD experiments (180-500 °C) of samples reduced at 350 °C.<sup>(f)</sup> CO<sub>2</sub> TPD experiments (50-850 °C) of samples reduced at 350 °C.<sup>(g)</sup> Temperature maxima of the peak as determined by TPD experiments.

\* Micropore volume and BEA framework pore size.

of the acid sites. In case of the latter, a significant content in basic sites was also established by CO<sub>2</sub> desorption analysis (0.160 meq CO<sub>2</sub>·g<sup>-1</sup>), mostly corresponding to the presence of weak basicity (110 °C). As expected, the highest basicity is exhibited by Pt/HTC (0.796 meq CO<sub>2</sub>·g<sup>-1</sup>), which indicates the major basic character of this material.

Regarding the size and dispersion of platinum particles, Table 2 shows important differences in these values among the studied catalysts. Both parameters are essential features in bifunctional catalysts, since their activities and selectivities are not only influenced by the nature of the metal species, but can also be controlled by their size and distribution.<sup>25,26,28</sup> As expected, a noticeable dispersion was found for catalysts with the highest specific surface, i.e. Pt/Beta and Pt/Al-SBA-15 (34.6 and 65.3 %, respectively), while Pt/SiO<sub>2</sub>, which shows the lowest BET surface area, has a very low metal dispersion (0.8 %). These values imply great differences in Pt particle sizes, ranging from 1.7 nm for Pt/Al-SBA-15 to 141 nm for Pt/SiO<sub>2</sub>. Equally, the presence of Brønsted acid sites in Pt/Beta and Pt/Al-SBA-15 may enhanced the Pt dispersion due to stronger interaction between the metal phase and the support.<sup>29</sup> The last aspect may also be responsible for the significant degree of dispersion and small particle size observed in case of Pt/WO<sub>3</sub>-ZrO<sub>2</sub> (41.4 % and 2.7 nm). Nevertheless, the lower metal loading of this catalysts may have affected these values. In this sense, Pt/Al<sub>2</sub>O<sub>3</sub>, Pt/TiO<sub>2</sub> and Pt/HTC show higher values of Pt particle sizes (7.7-29.4 nm), likely due to the combination of higher metal loading, middle textural properties and lower acid character. Finally, the estimated active metal surface areas may constitute a useful parameter for the evaluation of the studied catalytic activities.

### Conversion of furfural acetone condensation products.

A series of preliminary tests was performed in order to establish the most appropriate conditions for the hydrodeoxygenation experiments. Despite the exothermic character of the hydrogenation reactions, an increase in reactants conversion was observed with the increasing reaction temperature, within the experimental range. A

maximum temperature of 200 °C was set in order to keep the reactants and products in liquid phase. In addition, harsher conditions (>200 °C) led to undesirable severe C-C bond cleavage and coke formation, making the whole process less energy-efficient. During the course of the reaction, hydrogen was consumed and, consequently, more was supplied to maintain the pressure constant. The selected pressure value (50 bar) ensures excess of hydrogen during the whole course of the experiment. The amount of catalyst (1 g) and overall reaction time (480 min) were also optimized to observe significant changes in the product distribution. The results of these initial studies allowed defining a standard reaction procedure (described in section 2.4) for all the subsequent experiments presented in this work.

Figure 1 shows the variations in the relative molar concentration (X<sub>i</sub>%) of the main components of the feedstock (Table 1) as a function of the reaction time. Due to the significant differences in the molar fraction concentrations between these compounds, the results depicted in Figure 1 are referred to by their percentage variation (relative concentration) with the purpose of appreciate more clearly their evolution along reaction time. Most of the reactants show a decreasing tendency as a result of the progressive hydrogenation of their bonds (aliphatic C=C, ketonic C=O and furanic C=C). The highest rate of conversion for all tested catalysts corresponded to the compound F<sub>2</sub>-Ac, which in the experiments carried out with Pt/Al<sub>2</sub>O<sub>3</sub> and Pt/TiO<sub>2</sub> completely disappeared after 120 min. Similar behaviour was observed for F-Ac, F<sub>2</sub>-Ac<sub>2</sub> and F<sub>2</sub>-Ac<sub>3</sub>, showing a continuous decrease in their molar fractions as the reaction proceeded, although with a lower hydrogenation rate. Thus, except Pt/SiO<sub>2</sub>, the relative concentration values of these reactants after 480 min were close to zero, indicating an almost full conversion to hydrogenated compounds. The lowest hydrogenation rate of Pt/SiO<sub>2</sub> may be associated with the absence of acid/basic sites, as well as with its low active metal surface area (0.01 m<sup>2</sup>·g<sup>-1</sup>), which implies a poor hydrogenation activity. Likewise, the significant value of X<sub>i</sub>% observed for F<sub>2</sub>-Ac<sub>3</sub> after 480 min when using Pt/Beta catalyst (13.3 X<sub>i</sub>%) is very likely related to the steric limitations in microporous materials for bulky molecules such as F<sub>2</sub>-Ac<sub>3</sub>. Thus, in spite of most

of the Pt particles are probably located on the external surface, the lower accessibility to acid sites reduces the activity of this catalyst. In this respect, the kinetic curves observed for Pt/TiO<sub>2</sub> demonstrate clearly that large pores (mean pore size ≈ 300 Å) facilitate access of reactants to the active sites. The influence of mass transfer

limitations on the reaction was minimized by applying suitable experimental conditions as those suggested in a similar process,<sup>30</sup> as well as by using small catalyst particles (<100 μm) and vigorous stirring (1000 rpm).

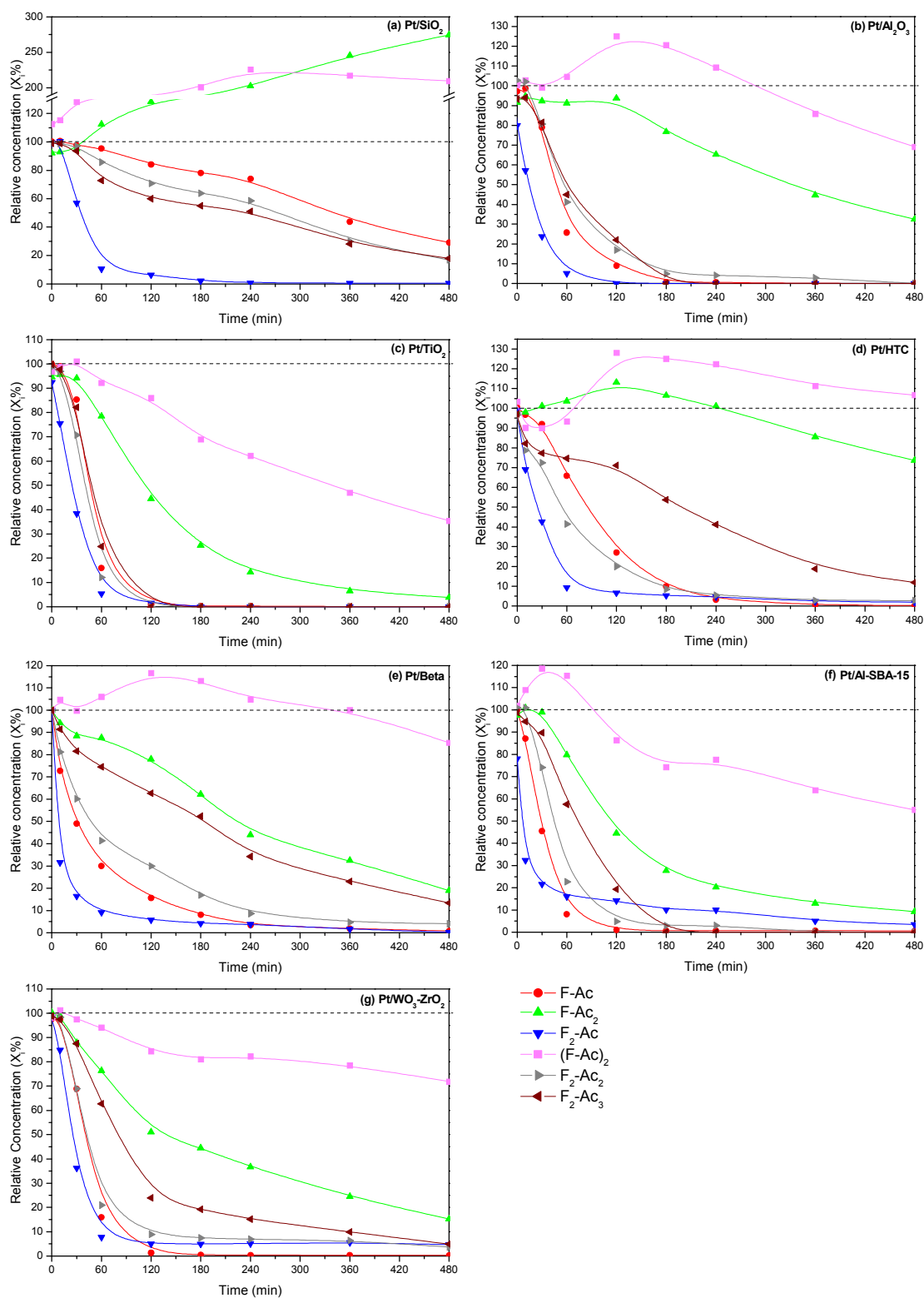


**Fig. 1** Evolution of the relative concentration ( $X_i\%$ ) of the reactants (furfural acetone condensation products) during the hydrodeoxygenation over different catalysts ( $T=200\text{ }^\circ\text{C}$ ;  $P=50\text{ bar}$ ;  $t=480\text{ min}$ )

The active metal surface area does not correlate with the initial hydrogenation conversion rate of the reactants. For example, for Pt/Beta and Pt/Al-SBA-15, which showed considerably high active metal surface areas (0.42 and 0.47 m<sup>2</sup>·g<sup>-1</sup>, respectively), presented similar or even lower conversion rates than the rest of the studied catalysts. This fact may be to the participation of acid/basic sites in the initial reactant conversion or to the plausibly different structure of Pt particles due to their different size and location.

On the other hand, the extent of the hydrogenation of F-Ac<sub>2</sub> and (F-Ac)<sub>2</sub> seems to be limited, even showing an increase in their relative molar fractions after 480 min when using Pt/SiO<sub>2</sub>. This fact may be associated with the formation of these compounds, due to the consecutive aldol condensation reactions of acetone with F-Ac or self-condensation of F-Ac. In the case of some other catalysts, like Pt/Al<sub>2</sub>O<sub>3</sub>, Pt/HTC, Pt/Beta and Pt/Al-SBA-15, the concentration of (F-Ac)<sub>2</sub> shows a maximum at short reaction times (60-120min). This behaviour indicates that these condensation reactions are faster than the hydrogenation of these reactants over fresh catalysts. The formation of F-Ac<sub>2</sub> and (F-Ac)<sub>2</sub> is observed even on Pt/SiO<sub>2</sub>, i.e. in absence of acid and basic sites, which implies that the condensation of F-Ac adducts takes place probably through a thermal route. Due to the poor hydrogenation performance of this catalyst (caused by the low specific surface of Pt), the consecutive conversion of these condensation products is only partial.

The extent of aldol condensation reactions over the studied catalysts is evidenced by the increasing concentration of diacetone alcohol (DAA) formed by acetone self-condensation. Subsequently, DAA undergoes successive dehydration and hydrogenation reactions yielding mesityl oxide (MSO), methyl isobutene ketone (MIBK) and methyl isobutyl carbinol (MIBC). This conversion process is schematically depicted in Figure 2, along with the variation of the concentration of these products in one of the performed experiments. Importantly, direct hydrogenation of acetone to isopropanol was not observed. Since the concentration of MIBK was increasing in all experiments as the reaction progressed and, DAA and MSO showed a maximum in their concentration, it can be inferred that the rate of the selective hydrogenation of DAA and MSO is faster than the rate of formation of MIBK, under the given

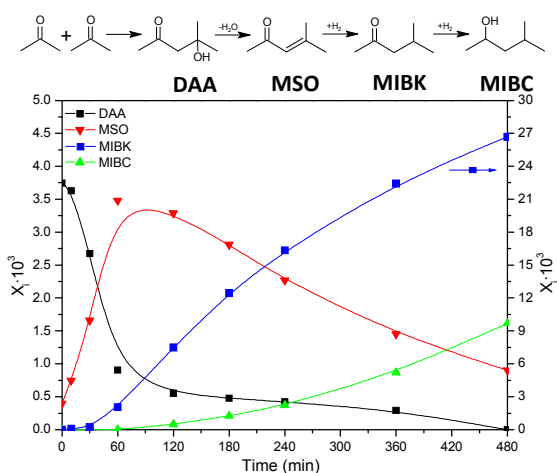


**Fig. 2** Aldol condensation and further hydrogenation of acetone itself (T=200 °C; P=50 bar; t=480 min)

experimental conditions. It is interesting to note that no higher molecular-weight products, such as dimethyl heptanone, derived from further condensation of acetone with MIBK were observed.

The motivation for performing hydrogenation/deoxygenation in presence of acetone is to couple aldol condensation of furfural with acetone with the subsequent hydrogenation without any intermediate separation steps, such as distillation of solvents that might be very demanding due to the high reactivity of the aldol condensation products. Although it is not the main objective of this work to analyse the influence of the tested catalysts on acetone conversion, it is worthy to mention that Pt/Beta, Pt/Al-SBA-15 and Pt/WO<sub>3</sub>-ZrO<sub>2</sub> gave the highest yield of MIBK. This result indicates a direct relation between the acidity of the used catalysts and the extent of the acetone self-condensation and consecutive hydrogenation represented in Figure 2.

### Hydrodeoxygenation selectivity.

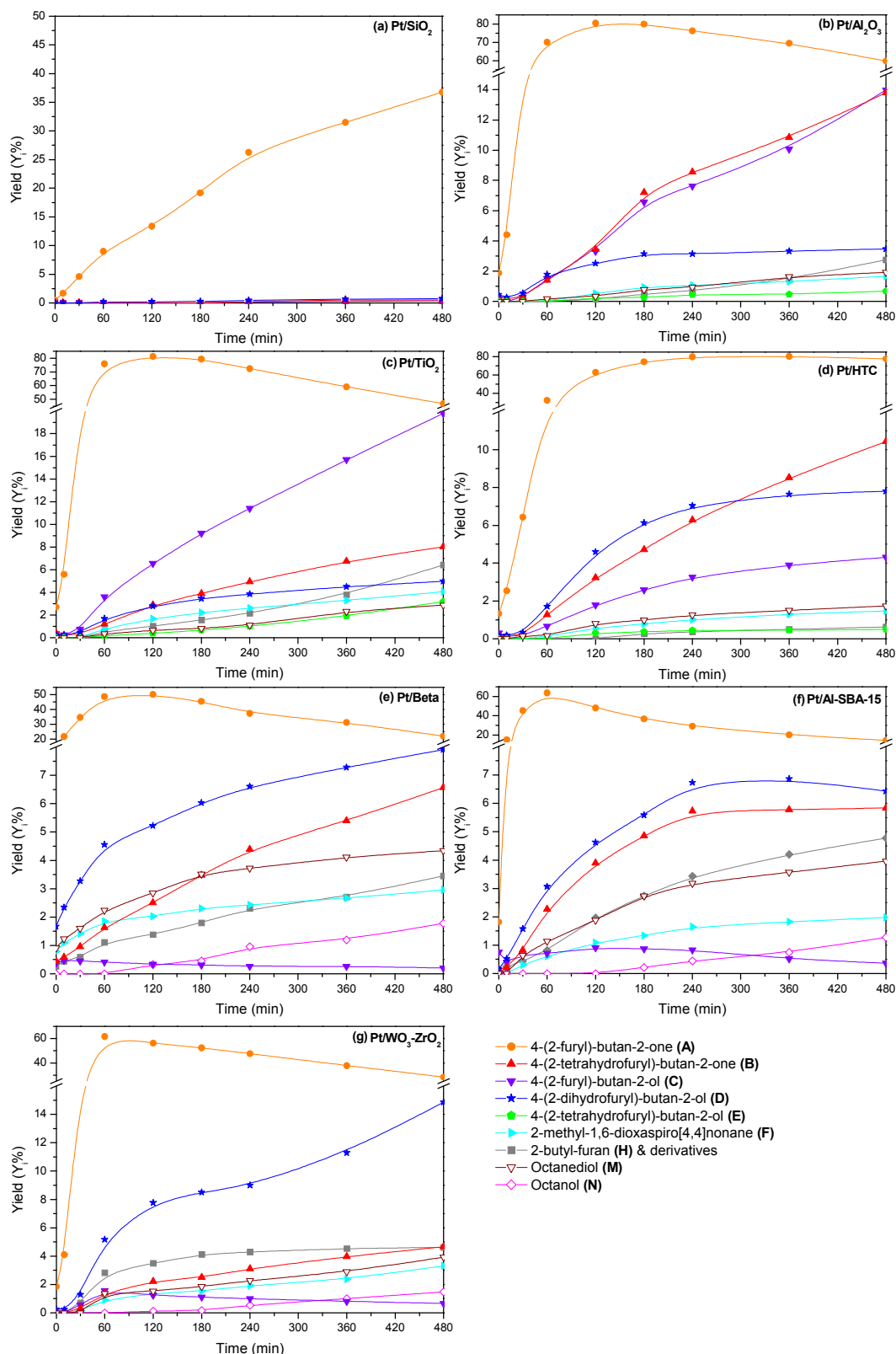
The multicomponent nature of the initial feedstock led to a complex mixture of products, derived from the successive hydrogenation steps of the different bonds (aliphatic C=C, furanic C=C and ketonic C=O), ring opening and dehydration reactions. Furthermore, some additional side reactions such as condensation, isomerization or cyclization may occur, resulting in a diverse product distribution within a wide range of molecular weights. Therefore, in order to simplify the discussion, the GC and GC-MS analyses of the collected samples were focused on the fraction of compounds originated from 4-(2-furyl)-3-buten-2-one (F-Ac), which constituted 72 % of the reactants (without taking into consideration acetone). The study of the reaction pathways of F-Ac transformation can be used as a case study for the estimation of the conversion pathways of the heavier furfural-acetone condensation products.

Figure 3 depicts the yields of the main products obtained from the hydrogenation of F-Ac as a function of reaction time for the different studied catalysts. In all cases, the high yield of 4-(2-furyl)-butan-2-one (A) stands out among the other hydrogenated products. The yield of this compound reaches a maximum at short reaction times, followed by a smooth decrease as it is consumed to afford more deeply hydrogenated products. This fact suggests that the hydrogenation of this conjugated C=C bond is very fast, whereas the further hydrogenation steps, i.e. of the ketone group and furan ring, are the rate determining hydrogenation steps. This behaviour is common for all tested catalysts except for Pt/SiO<sub>2</sub>, which shows a slow and continuous increase in the yield of A, indicating again the very poor hydrogenation performance of this material. This observation is also confirmed by the absence of the other intermediate products resulting from the consecutive hydrogenation of A in Pt/SiO<sub>2</sub> experiments.

The consecutive formation of hydrogenated compounds from the primary product (A) was also observed although in a lower extent. These included products such as 4-(2-tetrahydrofuryl)-butan-2-one (B) and 4-(2-furyl)-butan-2-ol (C), which are derived from furanic ring and ketonic bond hydrogenation, respectively. For some catalysts, like Pt/Al<sub>2</sub>O<sub>3</sub> and Pt/TiO<sub>2</sub>, the yield of these products reached significant values, >7.9 %, through a continuous increase as the reaction proceeded. However, in case of Pt/Beta, Pt/Al-SBA-15

and Pt/WO<sub>3</sub>-ZrO<sub>2</sub> the formation of **C** seems to be limited, not exceeding yields of 0.7 %. This fact may be correlated with a faster transformation of **C** into 4-(2-dihydrofuryl)-butan-2-ol (**D**) and 2-butyl-furan (**H**), via partial hydrogenation of the furan ring and

deoxygenation, respectively. The formation of **D** may be promoted by the smaller particle sizes observed in those catalyst, which may modify the surface chemical adsorption of the reactant and the subsequent hydrogenation steps.<sup>25,31</sup>



**Fig. 3** Evolution of the yield (Y%) of F-Ac hydrodeoxygenated products over different catalysts (T=200 °C; P=50 bar; t=480 min)

Thus, smaller Pt particles may favoured the interactions with the furanic ring, allowing the unconstrained adsorption of the most accessible double bond.<sup>22,32</sup> On the other hand, the higher acidic character showed by Pt/Beta, Pt/Al-SBA-15 and Pt/WO<sub>3</sub>-ZrO<sub>2</sub> may have enhanced deoxygenation reactions, increasing the formation of **H** (3.4-4.8 %). Overall, it is concluded that the selectivity to **C** decreased due to the combination of smaller Pt particle and the presence of acid sites.

The complete hydrogenation of the original molecule (F-Ac) led to the production of 4-(2-tetrahydrofuryl)-butan-2-ol (**E**), which only appeared in limited yields (<3.2 %). The low formation of this product might be related to the slower kinetics of furanic ring and ketonic bond hydrogenation, but also to the higher reactivity of their precursors, promoting side reactions which reduce the selectivity to this compound. On the other hand, the continuous increase in the yield of **E** can be explained by its higher stability, caused by the limitation of ring-opening steps of the saturated ring.<sup>33</sup> Among the mentioned side reactions, the formation of 2-methyl-1,6-dioxaspiro[4,4]nonane (**F**) took place, likely through the intramolecular addition of the hydroxyl group on the double bond of **D**.<sup>34</sup>

The extent of oxygen removal steps was confirmed by the formation of compounds such as 2-butyl-furan (**H**), 2-butyl-dihydrofuran (**I**), 2-propyl-tetrahydropyran (**J**) or 2-butyl-tetrahydrofuran (**K**). The deoxygenation steps took place mostly through dehydration or hydrogenolysis reactions which usually imply the interaction of Brønsted acid sites with the hydroxyl group.<sup>35</sup> Thus, the yield of deoxygenated compounds reached higher values with those catalysts that exhibited stronger acidity, like Pt/Beta, Pt/Al-SBA-15 and Pt/WO<sub>3</sub>-ZrO<sub>2</sub> (Figure 4a). In contrast, low acid materials or no-acid materials, such as Pt/Al<sub>2</sub>O<sub>3</sub> and Pt/HTC, respectively, show a lower extent of deoxygenation steps. However, Pt/TiO<sub>2</sub> exhibited also a remarkable deoxygenation activity indicating that even mild acidity together with improved accessibility is equally important for furanic ring interaction with the active sites.

The formation of linear alcohols like octanediols (**M**) and octanols (**N**) occurs via ring opening reactions through hydrogenolysis of a C-O bond of the furanic ring, leading to the formation of a new hydroxyl groups. The significant yields of octanediols at short reaction times (<60 min) in case of Pt/Beta, Pt/Al-SBA-15 and Pt/WO<sub>3</sub>-ZrO<sub>2</sub>, indicate that the formation of octanediols likely occurs through ring opening

of the primary intermediates, like **C**, since the yield of further hydrogenated precursors (**B**, **D** and **E**) are too low or non-existent at the beginning of the reactions. This observation is in accordance with Vlachos et. al.,<sup>36</sup> who reported that the ring opening reactions take preferentially place through non-saturated rings because of the higher energy barriers associated with ring opening of **D**, **B** and **E**. This behaviour may also be related with the observed low concentration of **C** with Pt/Beta, Pt/Al-SBA-15 and Pt/WO<sub>3</sub>-ZrO<sub>2</sub>, since in presence of acid sites the hydrogenolysis of the C-O bond of non-saturated furanic ring is promoted. Similar behaviour is observed in the production of octanols (**M**), whose yields seem to be linked to the formation of **H** (2-butyl-furan) and enhanced by the presence of acid sites (Pt/Beta, Pt/Al-SBA-15 and Pt/WO<sub>3</sub>-ZrO<sub>2</sub>). Figure 4b shows the variation in the yield of octanediols and octanols with reaction time for all studied catalysts. The continuous increase in the yield of linear alcohols implies that dehydration/hydrogenolysis could be the rate determining step in the conversion pathway to octane over the investigated set of platinum-containing catalysts.

### Proposal of a reaction scheme.

To shed light on the transformation pathways of furfural-acetone condensation products into hydrocarbons and to understand the role of different catalyst functionalities, an analysis of the kinetic curves exhibited in Figure 3 and in previously published work,<sup>14,17</sup> was performed. As a result a reaction scheme has been proposed to describe, in the most simplified way possible, the major routes in the conversion of 4-(2-furyl)-3-buten-2-one (F-Ac) into n-octane. The reaction scheme of the studied transformation is rather complicated, since it includes numerous intermediate products, side reactions, competitive and non-competitive steps, adsorption of solvent, formation of coke, etc. The product distribution consists of a mixture of compounds with different degrees of hydrogenation, indicating that there is a step by step mechanism through which various intermediates are formed. Figure 5 shows the essential features of the reaction pathway for the production of octane from F-Ac, comprising hydrogenation, condensation, isomerization, cyclization and dehydration/hydrogenolysis steps. Likewise, Table 3 displays the yield of F-Ac hydrogenated products obtained after 480 min, using the different prepared catalysts and the experimental procedure describe above.

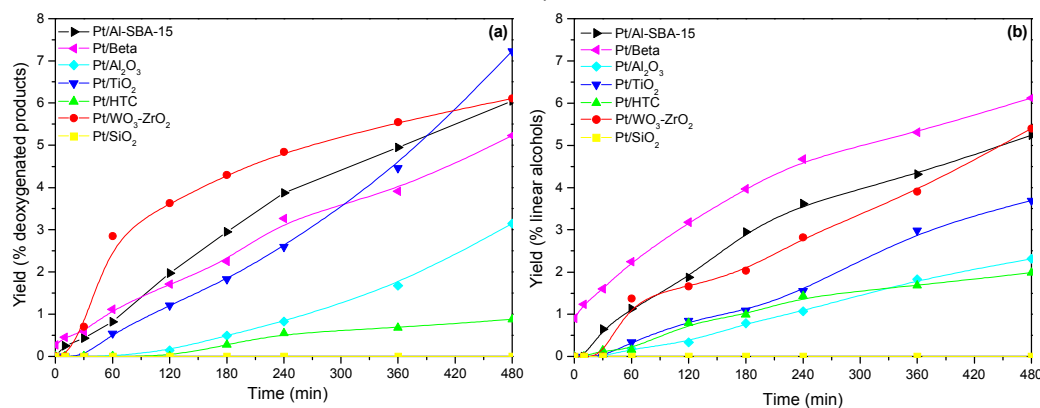


**Fig. 4** Evolution of the yield ( $Y_i$ %) of (a) deoxygenated products (**H+I+J+K+N**) and (b) linear alcohol products (**M+N**), from the hydrodeoxygenation of F-Ac over different catalyst ( $T=200\text{ }^\circ\text{C}$ ;  $P=50\text{ bar}$ ; 480 min)

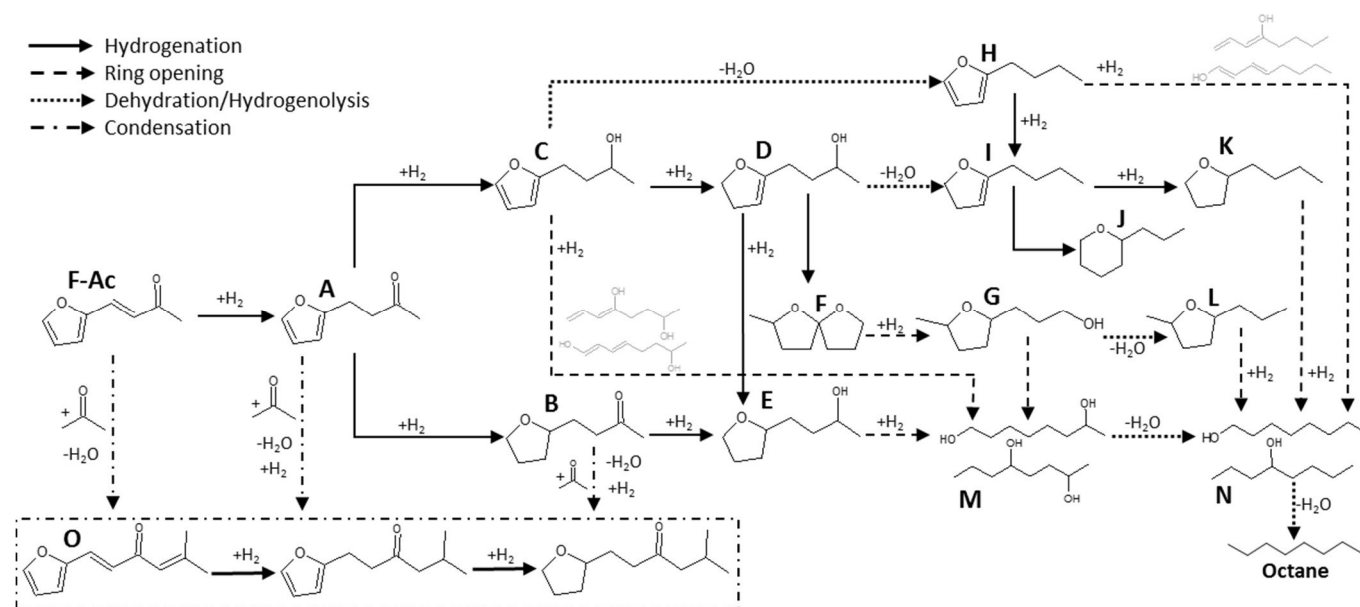


Fig. 5 Proposed reaction scheme for the hydrodeoxygenation of 4-(2-furyl)-3-buten-2-one (F-Ac) into octane

Firstly, the hydrogenation of the aliphatic C=C bond takes place yielding 4-(2-furyl)-butan-2-one (A). The fast hydrogenation of this bond is enhanced by its favourable thermodynamic conditions, and also due to the absence of steric limitations, unlike the case of the furanic ring bonds.<sup>19</sup> The subsequent hydrogenation of A may proceed by two parallel routes: hydrogenation of the ketonic C=O bond or hydrogenation of the furanic ring C=C bonds. The latter yields 4-(2-tetrahydrofuryl)-butan-2-one (B), which is an intermediate of the completely hydrogenated molecule 4-(2-tetrahydrofuryl)-butan-2-ol (E). The former affords 4-(2-furyl)-butan-2-ol (C) that can undergo many different side reactions in addition to its transformation into E. The yield of this intermediate furan alcohol (C) is very low (negligible) when using acid catalysts (Pt/Beta, Pt/Al-SBA-15 and Pt/WO<sub>3</sub>-ZrO<sub>2</sub>), most likely as a result of its immediate consumption yielding D, H and M. Specifically, the initial hydrogenation of the furanic ring of C produces a reactive intermediate, 4-(2-dihydrofuryl)-butan-2-ol (D), which may undergo

cyclization due to the interaction between the -OH group and the partially hydrogenated ring yielding 2-methyl-1,6-dioxaspiro[4,4]nonane (F).<sup>34</sup> In addition, D may undergo hydrogenation of the remaining double bond in the furanic ring, yielding thus E, or dehydration reactions forming 2-butyl-dihydrofuran (I). Similar step may occur directly from C, yielding 2-butyl-furan (H), which can be further hydrogenated to I. Alternatively, the furan C-O bond present in C may be hydrogenolysed resulting in opening of the furanic ring. This option yields linear unsaturated octanediols, which are rapidly hydrogenated to saturated octanediols (M). Otherwise, the formation of M can also occur via opening ring of E or 5-methyl-2-tetrahydrofuranpropanol (G), affording saturated octanediols directly. The latter derived from ring opening steps of F, via hydrogenolysis of one of the C-O bonds. In this respect, C-C bond scission is generally unfavourable upon ring opening via C-O bond cleavage.<sup>36,37</sup>

Table 3 4-(2-furyl)-3-buten-2-one (F-Ac) hydrodeoxygenation products after 480 min at 200 °C and 50 bar

Catalysts	Yield (Y <sub>i</sub> %)													
	F-Ac	A	B	C	D	E	F	G	H	I	J	M	N	O
Pt/ SiO <sub>2</sub>	29.2	36.7	0.5	0.4	0.7	-	-	-	-	-	-	-	-	12.7
Pt/Al <sub>2</sub> O <sub>3</sub>	0	59.7	13.8	14.0	3.5	0.8	1.6	1.4	-	0.2	2.7	1.9	0.4	-
Pt/TiO <sub>2</sub>	0	46.4	7.9	19.6	5.0	3.2	4.0	3.4	-	0.6	6.3	2.9	0.8	0.0
Pt/HTC	0.2	74.0	9.9	4.1	7.4	0.5	1.4	-	0.6	-	-	1.6	0.2	0.0
Pt/Beta	0.8	22.0	6.5	0.2	7.9	0.3	2.9	-	3.4	-	-	4.3	1.8	32.9
Pt/Al-SBA-15	0.6	14.2	5.8	0.3	6.4	0.6	2.0	1.2	4.8	-	-	4.0	1.3	39.7
Pt/WO <sub>3</sub> -ZrO <sub>2</sub>	0.2	28.3	4.7	0.7	14.7	1.1	3.3	2.2	4.6	0.3	-	3.9	1.5	34.6

\* 4-(2-furyl)-butan-2-one (A), 4-(2-tetrahydrofuryl)-butan-2-one (B), 4-(2-furyl)-butan-2-ol (C), 4-(2-dihydrofuryl)-butan-2-ol (D), 4-(2-tetrahydrofuryl)-butan-2-ol (E), 2-methyl-1,6-dioxaspiro[4,4]nonane (F), 5-methyl-2-tetrahydrofuranpropanol (G), 2-butyl-furan (H), 2-butyl-dihydrofuran (I), 2-propyl-tetrahydropyran (J), 2-butyl-tetrahydrofuran (K), 2-methyl-5-propyl-tetrahydrofuran (L), octanediols (M), octanols (N) and heavier condensation products (O).

The formation of **H** and **I** are a consequence of dehydration of the primary intermediates. This reaction implies the formation of water through the loss of -OH group from **C** or **D** intermediates. However, in case of Pt/Al<sub>2</sub>O<sub>3</sub> and Pt/TiO<sub>2</sub> the presence of **H** is a bit controversial, since although it is clearly observed at short reaction times, as the reaction progresses the GC retention time of the peak decreases gradually (i.e. **H** is co-eluting with a product of consecutive reactions and is itself consumed in the course of the reaction). According to the GC-MS pattern the co-eluting compound is 2-propyl-tetrahydropyran (**J**) and it seems to be formed at the expense of **H**, likely via a fast formation of **I**.<sup>38</sup> The reason for the significant yield of **J** over TiO<sub>2</sub> and Al<sub>2</sub>O<sub>3</sub> supported Pt is not yet fully understood. Nonetheless, the formation of **J** have been reported in similar processes by other authors, who have suggested its formation via isomerization and hydrogenation of **H**.<sup>13,39</sup> From the point of view of our results, the production of **J** seems to be linked to the presence of 2-butyl-dihydrofuran (**I**), since both products are obtained in the same experiments, suggesting that their formation by hydrogenation of **H** are closely related. On the other hand, the absence of **J** with the more acidic materials (Pt/Beta, Pt/Al-SBA-15 and Pt/WO<sub>3</sub>-ZrO<sub>2</sub>) indicate that with these catalysts the ring opening of **H** to form octanols (**N**) is more favoured by the presence of Brønsted acidity. In any case, the formation of **J** constitutes an undesired side reaction since it reduces the selectivity to octane by forming a stable compound. Despite some oxygen removal steps (deoxygenation) took place, the dehydration of octanediols and octanols towards octane was very restricted since the presence of the hydrocarbon was not detected by GC-MS analyses. Therefore, it is also likely that the formation of **N** take places mostly through **H** rather than by dehydration of **M**.

In addition to the hydrogenation route of F-Ac, the significant formation of heavier products (**O**) catalyzed by Pt/SiO<sub>2</sub>, Pt/Beta, Pt/Al-SBA-15 and Pt/WO<sub>3</sub>-ZrO<sub>2</sub> was observed. These compounds are products of aldol condensation of acetone either with F-Ac, or with other intermediate ketone compounds such as **A** and **B**. Thus, this route leads to the formation of longer carbon chain intermediates which, once deoxygenated, would ultimately yield larger alkenes (C<sub>11+</sub>), i.e. the overall hydrocarbon yield would not be affected in case of total hydrodeoxygenation. However, it should be considered that these reactions may lead to the production of a heavy fraction that can be involved in the formation of carbon deposits. Therefore, this aspect must be taken into consideration for the performance of longer experiments as a possible cause of catalyst deactivation. Likewise, the successive hydrogenation steps of **O** indicate the possibility to perform simultaneously aldol-condensation and hydrogenation reactions, although this process is technically very demanding since the optimal conditions for both reactions are different.<sup>40</sup> Particularly in case of acid catalysts, the yields of these heavier products were very significant (32.9-39.7 %), reducing thus considerably the maximum attainable selectivity to octane. One possibility to prevent these side reactions, is the use of other solvents than acetone (e.g. alcohols), which can be expected to limit the extent of aldol condensation reactions. It is also worth to note that despite almost one third of F-Ac undergoes further condensation, Pt/Beta, Pt/Al-SBA-15 and Pt/WO<sub>3</sub>-ZrO<sub>2</sub> afford the highest yield of octanols (1.3-1.8 %) among the studied catalysts. This indicates

superior ring opening and deoxygenation activity of platinum supported on acid supports in comparison with platinum on non-acidic or basic supports.

The above mentioned results suggest that employing acid catalysts, such as Pt/Beta, Pt/Al-SBA-15 and Pt/WO<sub>3</sub>-ZrO<sub>2</sub>, with hydrogenated intermediate products (i.e. products less prone to condensation), may improve the final yield of linear alcohols and octane. Hence, an additional longer experiment (16 h) was carried out consisting of two stages. Firstly, an 8 hours reaction was performed using Pt/TiO<sub>2</sub> and the original feedstock (Table 1). Secondly, Pt/Al-SBA-15 was added to the obtained product from the first stage and the experiment continued for another 8 hours. In this way the good hydrogenation activity of Pt/TiO<sub>2</sub> was combined with the good deoxygenation activity of Pt/Al-SBA-15. At the same time, it was expected that the decrease in the concentration of F-Ac and intermediates **A** and **B** during the first stage would limit the extent of acetone condensation reactions, and favour a higher yield of C<sub>8</sub> intermediates. The yields of products are shown in Figure 6 as a function of reaction time.

In line with the previous results, **A** and **C** are the main products obtained as a result of hydrogenation of F-Ac on Pt/TiO<sub>2</sub>. Both of the products are rapidly consumed when Pt/Al-SBA-15 is used as a catalyst. In case of **C**, which is completely absent at the end of the reaction (960 h), it is mostly due to the high promotion of ring opening and dehydration steps in presence of Brønsted acid sites, yielding **M** (19.7 %) and **H**, respectively. The latter is also fast converted to **J** (23 %) and **K** (10.8 %), via hydrogenation and isomerization reactions. The increasing amount of these products, together with **G**, indicates a significant limitation for opening saturated rings. Similarly, despite the high increase in **M**, the yield of **E** does not show any decrease, confirming the lower reactivity of this compound. Thus, in order to optimize the production of octane, the formation of fully hydrogenated species, such as **E**, should be avoided due to the more demanding conditions required to open their tetrahydrofuran ring in comparison with furan and dihydrofuran rings.

Figure 6 also reveals the intermediate character of the compound **B** and **D** showing a decreasing trend when the concentration of their respectively precursors (**A** and **C**) are too low. The formation of heavier products with Pt/Al-SBA-15 is not completely inhibited (**O**=6 %), due to the extent of condensation reactions between acetone and the remaining intermediate ketones, i.e. **A** and **B** after hydrogenation over Pt/TiO<sub>2</sub>. However, the yield of these compounds is considerably reduced in comparison with the experiment over Pt/Al-SBA-15 when F-Ac was used as feedstock, i.e. when F-Ac was in contact with the acid sites of Al-SBA-15 support. Consequently, the selectivity to C<sub>8</sub> intermediates that can be hydrodeoxygenated is enhanced, which together with the higher ring opening and dehydration activity of Pt/Al-SBA-15 lead to an increase in the formation of octanediols (19.7 %) and octanols (3.5 %).

The significantly higher concentration of octanediols (**M**) over octanols (**N**) suggests that the dehydration of linear alcohols is more restricted than furanic ring molecules. However, the higher hydrodeoxygenation rate achieved in the two stages experiment also afforded a low yield of octane (1.5 %), formed presumably by dehydration of **N**. The formation of green octane completes the

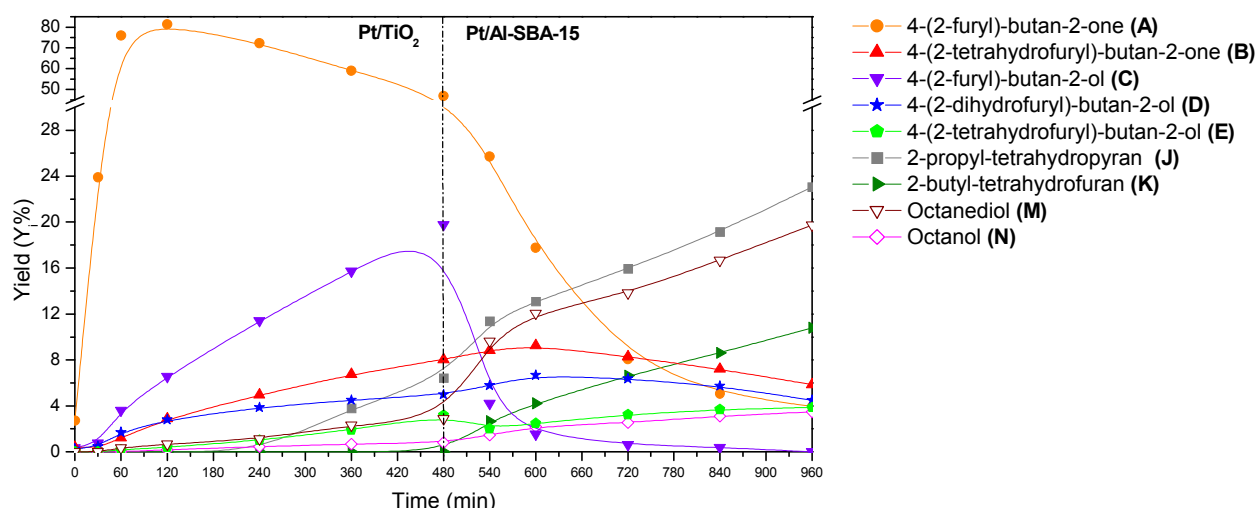


Fig. 6 Evolution of the yield ( $Y_i$ %) of F-Ac hydrogenated products ( $T=200\text{ }^\circ\text{C}$ ;  $P=50\text{ bar}$ ) in a two stages experiment: Pt/TiO<sub>2</sub> (8 h) and Pt/Al-SBA-15 (8 h)

proposed reaction scheme (Fig. 5), setting the groundwork for the future development of catalysts capable deoxygenate efficiently furfural condensation products in green hydrocarbons.

## Conclusions

The hydrodeoxygenation of furfural acetone condensation products has been studied using different supported Pt catalysts. The studied materials show a wide range of textural and acid properties which affect significantly the activity and selectivity of the process. The multicomponent nature of the initial feedstock (derived from furfural acetone aldol condensation experiments) led to a complex mixture of products, formed mainly by different extent of hydrogenation, ring opening and dehydration/hydrogenolysis reactions. Based on the study of the conversion rates and the kinetic behaviours showed by the main reactants and intermediates, a reaction scheme for the conversion of 4-(2-furyl)-3-buten-2-one (F-Ac) into octane has been proposed. The performed experiments indicated that conversion pathways and product distribution may be significantly modified by the catalytic properties of the studied supports.

Except Pt/SiO<sub>2</sub>, all catalysts showed a high conversion of the reactants, mostly due to the complete hydrogenation of the aliphatic C=C bonds. However, the extent of the conversion of furanic C=C and ketonic C=O bonds was more limited, particularly when using HTC and Al<sub>2</sub>O<sub>3</sub> as support. The use of Pt/TiO<sub>2</sub> promoted further hydrogenation, although the selectivity to linear alcohols seemed to be limited by the slow rate of dehydration and ring-opening steps. In all cases, ring-opening reactions occurred preferentially through non-saturated rings, indicating the possible convenience of a selective hydrogenation to aliphatic C=C and ketonic C=O bonds in the early steps. Likewise, in case of Pt supported over Beta, Al-SBA-15, WO<sub>3</sub>-ZrO<sub>2</sub> aldol condensation reactions took place between carbonyl containing intermediates and acetone, yielding longer carbon chain compounds. Although the formation of these molecules reduced the concentration of C<sub>8</sub> molecules, a remarkable

selectivity of linear alcohols was observed due to the higher extent of ring-opening and dehydration reactions in presence of Brønsted acid sites.

The production of octanols and octanediols having a potential as valuable petrochemical feedstocks was improved by performing a two stage experiments, using Pt/TiO<sub>2</sub> (8 h) and Pt/Al-SBA-15 (8 h). The further hydrogenation of the primary reactants using Pt/TiO<sub>2</sub>, along with the higher promotion of ring-opening and dehydration reactions with Pt/Al-SBA-15, enhanced the hydrodeoxygenation rate of C<sub>8</sub> intermediates, achieving a final production of an octane fraction.

## Acknowledgements

This publication is a result of the project no. P106/12/G015 supported by the Czech Science Foundation which is being carried out in the UniCRE center (CZ.1.05/2.1.00/03.0071) whose infrastructure was supported by the European Regional Development Fund and the state budget of the Czech Republic.

## Notes and references

- S. De, B. Saha and R. Luque, *Bioresource technology*, 2015, **178**, 108.
- J.J. Bozell and G. R. Petersen, *Green Chemistry*, 2010, **12**, 539.
- K. Yan, G. Wu, T. Lafleur and C. Jarvis, *Renewable and Sustainable Energy Reviews*, 2014, **38**, 663.
- K.J. Zeitsch, *The chemistry and technology of furfural and its many by-products (Vol. 13)*, Elsevier, 2000.
- S. Dutta, S. De, B. Saha and M.I. Alam, *Catalysis Science & Technology*, 2010, **2**(10), 2025.
- L. Faba, E. Díaz and S. Ordóñez, *Applied Catalysis B: Environmental*, 2012, **113**, 201.
- O. Kikhtyanin, V. Kelbichová, D. Vitvarová, M. Kubů and D. Kubička, *Catalysis Today*, 2014, **227**, 154.

8. L. Hora, V. Kelbichová, O. Kikhtyanin, O. Bortnovskiy and D. Kubička, *Catalysis Today*, 2014, **223**, 138.
9. J.N. Chheda and J.A. Dumesic, *Catalysis Today*, 2007, **123**(1), 59.
10. R. Xing, A.V. Subrahmanyam, H. Olcay, W. Qi, G.P. van Walsum, H. Pendse and G.W. Huber, *Green chemistry*, 2010, **12**(11), 1933.
11. H. van der Wal, B.L. Sperber, B. Houweling-Tan, R.R. Bakker, W. Brandenburg and A.M. López-Contreras, *Bioresource technology*, 2013, **128**, 431.
12. M. Gliński, J. Kijeński and A. Jakubowski, *Applied Catalysis A: General*, 1995, **128**(2), 209.
13. T.N. Pham, D. Shi, T., Sooknoi, and D.E. Resasco, *Journal of Catalysis*, 2012, **295**, 169.
14. W. Xu, Q. Xia, Y. Zhang, Y. Guo, Y. Wang and G. Lu, *ChemSusChem*, 2011, **4**(12), 1758.
15. Q.N. Xia, Q. Cuan, X.H. Liu, X.Q. Gong, G.Z. Lu and Y.Q. Wang, *Angewandte Chemie International Edition*, 2014, **53**(37), 9755.
16. L. Faba, E. Díaz, and S. Ordóñez, *Catalysis Science & Technology*, 2015, **5**(3), 1473.
17. L. Faba, E. Díaz, and S. Ordóñez, *Applied Catalysis B: Environmental*, 2014, **160**, 436.
18. W. Xu, X. Liu, J. Ren, P. Zhang, Y. Wang, Y. Guo and G. Lu, *Catalysis communications*, 2010, **11**(8), 721.
19. C.J. Barrett, J.N. Chheda, G.W. Huber and J.A. Dumesic, *Applied catalysis B: environmental*, 2006, **66**(1), 111.
20. A.D. Sutton, F. D. Waldie, R. Wu, M. Schlaf, A. Louis III and J.C. Gordon, *Nature chemistry*, 2013, **5**(5), 428.
21. R. Zanella, C. Louis, S. Giorgio and R. Touroude, *Journal of Catalysis*, 2004, **223**(2), 328.
22. M. Englisch, A. Jentys, and J.A. Lercher, *Journal of Catalysis*, 1997, **166**(1), 25.
23. T. B. L.W. Marinelli, J. H. Vleeming and V. Ponc, *Studies in Surface Science and Catalysis*, 1993, **75**, 1211.
24. J. Lee, Y. Xu, and G.W. Huber, *Applied Catalysis B: Environmental*, 2013, **140**, 98.
25. P. Claus, *Topics in Catalysis*, 1998, 5(1-4), 51.
26. P. Mäki-Arvela, J. Hajek, T. Salmi and D.Y. Murzin, *Applied Catalysis A: General*, 2005, **292**, 1.
27. O. Kikhtyanin, L. Hora and D. Kubička, *Catalysis Communications*, 2015, **58**, 89.
28. W. Zang, G. Li, L. Wang and X. Zhang, *Catalysis Science & Technology*, 2015, **5**(5), 2532.
29. B. Delmon, P. Grange, and G.F. Froment, *Hydrotreatment and hydrocracking of oil fractions*, Elsevier, 1997.
30. P.A. Ramachandran and R.V. Chaudhari, *Three-phase catalytic reactors (Vol. 2)*. Gordon & Breach Science Pub, 1983.
31. C.J. Kliewer, C. Aliaga, M. Bieri, W. Huang, C.K. Tsung, J.B. Wood, K. Komvopoulos and G. A. Somorjai, *Journal of the American Chemical Society*, 2010, **132**(37), 13088.
32. U.K. Singh and M. A. Vannice, *Studies in Surface Science and Catalysis*, 2000, **130**, 497.
33. S. Sitthisa and D.E. Resasco, *Catalysis letters*, 2011, **141**(6), 784
34. K. Alexander, L.S. Hafner and L. E Schniepp, *Journal of the American Chemical Society*, 1951, **73**(6), 2725.
35. P.M. Mortensen, J.D. Grunwaldt, P.A. Jensen and A.D. Jensen, *ACS Catalysis*, 2013, **3**(8), 1774.
36. S. Wang, V. Vorotnikov and D.G. Vlachos, *Green Chemistry*, 2014, **16**(2), 736.
37. C.R. Waidmann, A.W. Pierpont, E.R. Batista, J.C. Gordon, R.L. Martin, R.M. West and R. Wu, *Catalysis Science & Technology*, 2013, **3**(1), 106.
38. D. Robin, M. Sarraf, H.E. Audier and M. Fetizon, *Tetrahedron letters*, 1984, **25**(35), 3815.
39. K.L. Luska, J. Julis, E. Stavitski, D.N. Zakharov, A. Adams and W. Leitner, *Chemical Science*, 2014, **5**(12), 4895.
40. L. Faba, E. Díaz and S. Ordóñez, *ChemSusChem*, 2014, **7**, 2816.

